Measurement of the Initial Levels of DNA Damage in Human Lymphocytes Induced by 29 kV X Rays (Mammography X Rays) Relative to 220 kV X Rays and γ Rays

Author(s): M. Gomolka, U. Rössler, S. Hornhardt, L. Walsh, W. Panzer, and E. Schmid
Source: Radiation Research, 163(5):510-519.
Published By: Radiation Research Society
DOI: http://dx.doi.org/10.1667/RR3343
URL: http://www.bioone.org/doi/full/10.1667/RR3343

RADIATION RESEARCH **163**, 510–519 (2005)
0033-7587/05 $15.00

Measurement of the Initial Levels of DNA Damage in Human Lymphocytes Induced by 29 kV X Rays (Mammography X Rays) Relative to 220 kV X Rays and γ Rays

M. Gomolka,[a,1] U. Rössler,[a] S. Hornhardt,[a] L. Walsh,[b] W. Panzer[c] and E. Schmid[b,d]

[a] *Federal Office for Radiation Protection, Department of Radiation Protection and Health (SG1.1), 85764 Oberschleissheim, Germany;* [b] *Radiobiological Institute, University of Munich, 80336 Munich, Germany; and* [c] *Institute of Radiation Protection and* [d] *Institute of Radiobiology, GSF-National Research Center for Environment and Health, 85764 Neuherberg, Germany*

Gomolka, M., Rössler, U., Hornhardt, S., Walsh, L., Panzer, W. and Schmid, E. Measurement of the Initial Levels of DNA Damage in Human Lymphocytes Induced by 29 kV X Rays (Mammography X Rays) Relative to 220 kV X Rays and γ Rays. 163, 510–519 (2005).

Experiments using the alkaline comet assay, which measures all single-strand breaks regardless of their origin, were performed to evaluate the biological effectiveness of photons with different energies in causing these breaks. The aim was to measure human lymphocytes directly for DNA damage and subsequent repair kinetics induced by mammography 29 kV X rays relative to 220 kV X rays, ^{137}Cs γ rays and ^{60}Co γ rays. The level of DNA damage, predominantly due to single-strand breaks, was computed as the Olive tail moment or percentage DNA in the tail for different air kerma doses (0.5, 0.75, 1, 1.5, 2 and 3 Gy). Fifty cells were analyzed per slide with a semiautomatic imaging system. Data from five independent experiments were transformed to natural logarithms and fitted using a multiple linear regression analysis. Irradiations with the different photon energies were performed simultaneously for each experiment to minimize interexperimental variation. Blood from only one male and one female was used. The interexperimental variation and the influence of donor gender were negligible. In addition, repair kinetics and residual DNA damage after exposure to a dose of 3 Gy were evaluated in three independent experiments for different repair times (10, 20, 30 and 60 min). Data for the fraction of remaining damage were fitted to the simple function $F_d = A/(t + A)$, where F_d is the fraction of remaining damage, t is the time allowed for repair, and A (the only fit parameter) is the repair half-time. It was found that the comet assay data did not indicate any difference in the initial radiation damage produced by 29 kV X rays relative to the reference radiation types, 220 kV X rays and the γ rays of ^{137}Cs and ^{60}Co, either for the total dose range or in the low-dose range. These results are, with some restrictions, consistent with physical examinations and predictions concerning, for example, the assessment of the possible difference in effectiveness in causing strand breaks between mammography X rays and conventional (150–250 kV) X rays, indicating that differences in biological effects must arise through downstream processing of the damage.

INTRODUCTION

The dependence of the biological effects for different kinds of cell damage on photon energy is well documented. Cross comparisons of dose–response curves, which relate indicators of cellular damage such as chromosomal aberrations, mutation induction, cell survival and neoplastic cell transformation (in human and mouse cell lines) to absorbed doses of photons, e.g. at energies from 29 kV (mammography X rays) to about 200 kV (conventional X rays) or to 1.25 MeV (^{60}Co γ rays), have resulted in low-dose relative biological effectiveness (RBE) values ranging from 1 to 10 (*1–8*). However, it is uncertain whether the marked dependence of RBE on photon energy for these biological indicators is also representative of the complete biological effectiveness for the photon-induced initial DNA damage to late radiation effects in humans. This problem has gained particular attention with regard to risk–benefit considerations for mammography, because such findings are partly inconsistent with values predicted from microdosimetric analyses for the low-dose RBE of mammography radiation (*9–11*). Whereas conventional X rays interact with cellular systems through Compton electrons and photoelectrons, the 29 kV X rays interact primarily through the photoelectric effect. Due to the low energy of the 29 kV photons, low-energy secondary electrons are released, which leads not only to a different energy deposition pattern in the cellular system but also to greater biological effects than those produced by higher-energy photons. Physical models describing the possible energy deposition pattern in the DNA and the resulting DNA damage predict an RBE of only 1.3 with an upper limit no greater than about 2 for 29 kV X rays relative to conventional X rays (*9*).

The cellular damage indicators depend strongly on the mechanisms of biological cell responses after radiation damage, e.g. DNA repair and the induction of cell death by apoptosis or necrosis. The dose response for every bi-

[1] Address for correspondence: Federal Office for Radiation Protection, Department of Radiation Protection and Health (SG1.1), Ingolstädter Landstr. 1, 85764 Oberschleissheim, Germany; e-mail: mgomolka@bfs.de.

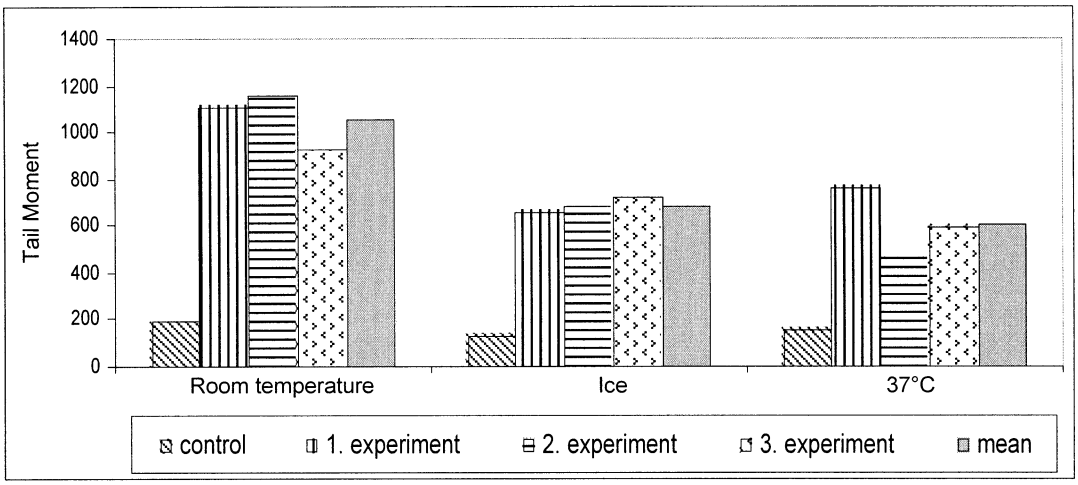

FIG. 1. Effect of temperature on damage induced during irradiation. Damage at room temperature (20°C) is increased compared to irradiation on ice or at 37°C.

ological indicator is an indirect measurement of the effect produced by the specific radiation type. The direct action of radiation on DNA can be detected by measuring single- or double-strand breaks or base changes caused by direct deposition of the radiation energy or by induced reactive oxygen species. Several techniques have been applied to study such radiation-induced DNA single-strand and/or double-strand breaks with different sensitivities to the specific lesions. These include alkaline or neutral filter elution (*12, 13*), alkaline unwinding (*14, 15*), sucrose gradient centrifugation (*16–18*), pulsed-field gel electrophoresis (*19–22*), and nucleoid sedimentation (*23, 24*). These techniques have the disadvantage that DNA damage is investigated in a population of cells and not at the single cell level.

The alkaline comet assay provides an excellent test for detecting direct DNA damage with respect to single-strand breaks, regardless of their origin, at the single cell level. In contrast to the neutral comet assay, which detects specifically double-strand breaks (DSBs), the alkaline assay is performed at doses that are relevant to physiological effects. It has been used widely to measure both *in vitro* and *in vivo* DNA damage and repair after the exposure of mammalian cells to various genotoxic agents such as chemicals and ionizing and non-ionizing radiation (*25–28*). For example, it has been reported that the alkaline comet assay is a useful biological technique to assess the biological effectiveness of different types of high-LET radiation such as neutrons (*29–32*). However, as recently observed for the induction of dicentric chromosomes in human lymphocytes (*33*), the RBE of neutrons depends on the choice of the low-LET reference radiation. So far no attempt has been made to test the usefulness of the alkaline comet assay for distinguishing between different types of low-LET radiation, which differ only slightly in energy deposition patterns.

Consequently, the purpose of the present study was to compare, in simultaneously performed comet assay experiments, both the initial radiation damage and the associated subsequent DNA temporal repair patterns induced by 29 kV X rays with those of their reference radiation types: 220 kV X rays, ^{137}Cs γ rays and ^{60}Co γ rays.

MATERIALS AND METHODS

For the present study, peripheral blood was taken with informed consent from two healthy donors: one male (age 64) and one female (age 38) donor. This was considered to be necessary for such a systematic investigation to minimize interindividual variations in sensitivity. All experiments were performed at room temperature (~20–22°C), because exact dosimetry for irradiation on ice with 29 kV X rays was not possible. However, a preliminary experiment showed that the magnitude of the initial DNA damage in human lymphocytes induced by 3 Gy of ^{60}Co γ rays at 37°C and 20°C and on ice was greatest at 20°C (Fig. 1). Therefore, it can be assumed that the DNA repair processes did not result in an underestimation of the initial DNA damage under the chosen temperature conditions. Irradiation was performed simultaneously with all four radiation sources per experimental set to decrease possible variations due to different experimental conditions. Immediately after irradiation, whole blood aliquots were set on ice prior to embedding the blood cells in agarose. To study DNA repair, blood samples were incubated at 37°C for defined times before setting them on ice.

Irradiation and Dosimetry

Due to dosimetric demands, the blood irradiation occurred in different blood containers. For the soft mammography X rays, the containers had to be very thin, with thin walls, to minimize the dose decrement within the blood volume and the distortion of the X-ray spectrum by the walls. For the highly energetic γ rays, secondary electron equilibrium had to be established. The air kerma rates were ~0.42 Gy/min for the X rays and ^{60}Co γ rays and ~0.66 Gy/min for the ^{137}Cs γ rays.

Mammography Radiation (29 kV, tungsten anode, 50 μm rhodium filtration)

The blood was irradiated in flat cylindrical containers (2.2 mm thick, 23.9 mm in diameter) with 20 μm polyethylene terephthalate (Mylar) windows at the entrance and exit side. To generate a typical radiation quality for mammography, a Dermopan soft X-ray therapy unit (Siemens) with an AEW50/25ö X-ray tube (anode material tungsten; anode angle

45°) was used. The unit was operated at a nominal tube voltage of 29 kV and a tube current of 20 mA. Since the Dermopan contains a rather basic one-peak high-voltage generator, with a strong dependence of tube voltage from primary voltage, tube current and duration of irradiation, tube current and primary voltage at the transformer were kept constant manually during irradiation. Under these conditions a tube voltage of 29 kV could be achieved, as determined by means of a high-purity germanium X-ray spectrometer. The beam filtration consisted of 1 mm beryllium (tube window) and 50 μm rhodium (Rh) (RH000210, Goodfellow). The X-ray spectrum, characterized by the rhodium K edge at 23.2 keV, had a mean photon energy of 19.4 keV and a half-value layer (HVL) of 0.51 mm aluminum, both values calculated from the photon spectrum. HVL values in mammography range are typically from 0.34 to 0.56 mm aluminum (*34*).

Two 0.02-cm³ soft X-ray chambers (type M 23342, PTW Company, Germany) were used for dosimetry. One, connected to an electrometer IQ4 (PTW) and mounted directly beside the blood container, served as a monitor chamber during irradiation. For the other chamber, connected to a Unidos electrometer (PTW), an air kerma calibration factor from PTB (German National Metrology Institute) for the quality T 30 (30 kV; 0.5 mm aluminum; E_m = 19.6 keV; HVL = 0.36 mm aluminum) was available. By means of this chamber, the monitor was calibrated in terms of air kerma at the container-to-focus distance (~15 cm). More details on the X-ray source and the dosimetric procedures were given by Göggelmann *et al.* (*4*).

The mean absorbed dose to blood, D_{blood}, was determined, using Eqs. (1) and (2), from the measured air kerma at the position of the entrance window (K_{entr}), measured air kerma behind the exit window (K_{exit}) and a backscatter factor (BSF = 1.033) calculated by Monte Carlo methods for the above, filled blood container and spectrum. (The calculation of BSF was performed by M. Zankl, GSF-Institute for Radiation Protection.)

$$D_{blood} = \frac{1}{2} \times (BSF \times K_{entr} + K_{exit}) \times \frac{\overline{(\mu_{en}/\rho)}_{blood}}{\overline{(\mu_{en}/\rho)}_{air}}; \quad (1)$$

$$D_{blood} = K_{air} \times 0.966; \quad (2)$$

where $\overline{(\mu_{en}/\rho)}_m$ is the mean spectral mass energy absorption coefficient for the materials *m* (blood, air). $\overline{(\mu_{en}/\rho)}_m$ was calculated using Eq. (3);

$$\overline{\left(\frac{\mu_{en}}{\rho}\right)}_m = \frac{\int_E \Phi(E) \times E \times [\mu_{en}(E)/\rho]_m \, dE}{\int_E \Phi(E) \times E \, dE}, \quad (3)$$

from the photon spectrum $\Phi(E)$ and fitted $(\mu_{en}(E)/\rho)_m$ values, taken from Hubbell (*35*).

Reference Radiation (220 kV, tungsten anode, 4.05 mm aluminum + 0.5 mm copper filtration)

The blood was irradiated in 1-ml syringes (7 mm in diameter). The reference radiation quality was generated by a highly stabilized MG 320 X-ray unit (Philips) with an MCN 323 X-ray tube (anode material tungsten; anode angle 22°) operated at a tube voltage of 220 kV and a tube current of 15 mA. The beam filtration consisted of a 3-mm beryllium (tube window) and 4.05 mm aluminum + 0.5 mm copper added filtration. The X-ray spectrum is characterized by a mean photon energy of 95.6 keV and a half-value layer of 1.39 mm copper; both values were calculated from the photon spectrum.

A transmission chamber (type 24366, PTW) connected to an IQ4 electrometer served as a monitor chamber. A 1-cm³ thimble chamber (type M23331, PTW) connected to a Unidos electrometer with an air kerma calibration factor from PTB for the quality T 200 (200 kV; 4 mm aluminum + 1 mm copper; HVL = 1.6 mm copper) was used to calibrate the monitor in terms of air kerma in the focus-to-syringe distance (70 cm).

Absorbed dose to blood was calculated from the measured air kerma according to

$$D_{blood} = K_{air} \times \frac{\overline{(\mu_{en}/\rho)}_{blood}}{\overline{(\mu_{en}/\rho)}_{air}} \times T; \quad (4)$$

$$D_{blood} = K_{air} \times 1.067; \quad (5)$$

where $\overline{(\mu_{en}/\rho)}_m$ is the mean spectral mass energy absorption coefficient, analogous to Eq. (3) (*35*), and T = 0.97 is a correction factor for the dose decrement within the syringe.

Reference Radiation (^{60}Co γ rays)

Blood samples were irradiated in 2-ml syringes (11 mm in diameter) in the center of a Perspex phantom (thickness 22 mm, width 70 mm, height 117 mm) at an Eldorado 78 therapy unit (Atomic Energy of Canada Ltd). Air kerma was measured by means of a 1-cm³ thimble chamber (type M23331, PTW) connected to a Unidos electrometer (PTW) in an identical phantom. For the chamber an air kerma calibration factor for ^{60}Co γ rays from PTB was available. Absorbed dose to blood was determined from measured air kerma in source-to-syringe distance (~160 cm) using Eqs. (6) and (7),

$$D_{blood} = K_{air} \times \frac{\overline{(\mu_{en}/\rho)}_{blood}}{\overline{(\mu_{en}/\rho)}_{air}}; \quad (6)$$

$$D_{blood} = K_{air} \times 1.102; \quad (7)$$

where $(\mu_{en}/\rho)_m$ is the mass energy absorption coefficient of blood and air for ^{60}Co γ rays (*35*).

Reference Radiation (^{137}Cs γ rays)

Blood (10 μl) was irradiated in 20-μl Eppendorf caps placed in a tart-shaped holder in a closed HWM D2000 irradiation facility (Wälischmiller). In spite of its unfavorable properties with regard to field homogeneity and consequently for dosimetry, this source was the only one available that provided dose rates similar to those of the other sources. For this source, an earlier calibration already existed already in terms of absorbed dose to water in the midline plane of the irradiation chamber of the source, where the Eppendorf caps were placed. Air kerma was determined by condenser-type chambers (PTW) evaluated with an integrating electrometer (Condiometer, PTW). The condenser chambers were again calibrated by means of a Farmer Dosimeter 2570 with a 0.6-cm³ thimble chamber (type 2571) at an open Caesa-Gammatron source (Siemens), and the results were converted into absorbed dose to water. A manufacturer's calibration existed for the ^{137}Cs ionization chamber.

Absorbed dose to blood was finally determined from absorbed dose in the midline plane using Eqs. (8) and (9):

$$D_{blood} = D_{water} \times \frac{\overline{(\mu_{en}/\rho)}_{blood}}{\overline{(\mu_{en}/\rho)}_{water}}; \quad (8)$$

$$D_{blood} = D_{water} \times 0.991. \quad (9)$$

Due to field inhomogeneity and the multiple steps involved, the error in the dose measurements for the ^{137}Cs γ radiation was 10%, whereas the errors for the three other radiation types were less than 3%.

DNA Repair

DNA repair was assessed by incubation of the samples at 37°C immediately after irradiation. Aliquots were taken after certain intervals, usually from 10 to 60 min after irradiation, and set on ice. In parallel, sham-irradiated controls were also collected after the same intervals.

Comet Assay

For the comet assay, a modification of the original protocol of Singh *et al.* (*36, 37*) was applied to whole blood. Special microscope slides

(ESW-370; Erie Scientific, Portsmouth, NH) with frosted edges and a clear window were precoated with 200 μl of 0.1% low-melting agarose (Sigma) and dried at 40°C on a warming plate. Then 10 μl of whole blood was mixed with 100 μl of 0.5% warm agarose (Amresco, Solon, OH) at 50°C and immediately transferred onto prewarmed precoated slides. A cover slip was placed gently over the agarose prior to chilling the slide for 5 min at 0°C on a cooling plate. For further treatment the cover slip was removed.

The microscope slides were immersed in a freshly prepared cold lysis buffer (2.5 *M* NaCl, 100 m*M* Na_4EDTA, pH 10, 10 m*M* Tris HCl, pH 10, 1% SDS, and 1% Triton X-100). Lysis was performed over night. Afterward, most nuclear proteins were removed by incubation in the second lysis buffer (2.5 *M* NaCl, 100 m*M* Na_4EDTA, pH 10, 10 m*M* Tris HCl, pH 10) for 1 h at 37°C. Slides were transferred to a specially adapted tray to prevent movement of slides during electrophoresis (Amersham Pharmacia HE100 Supersub). Twenty-one slides could be electrophoresed in one electrophoresis chamber. Unwinding was performed for 20 min in electrophoresis buffer (300 m*M* NaOH, 2% DMSO, and 10 m*M* Na_4EDTA, pH 10; pH >13). The temperature during electrophoresis (0.8 V/cm; 300 mA; 30 min) was kept constant at 20°C by a temperature control unit. After electrophoresis, the DNA was precipitated and fixed by incubation in 1% ammonium acetate in ethanol (5 ml of 10 *M* ammonium acetate and 45 ml of 100% ethanol) for 30 min at room temperature. After dehydration in 100% ethanol overnight, the slides were rehydrated with 70% ethanol for 5 min (to avoid the agarose cracking during drying), air-dried and stored at room temperature prior to staining. Slides were incubated for 15 min in double-distilled water and then stained with 50 μl of a solution containing 950 μl water, 60 μl DMSO, 200 μl Vectashield (Vector Laboratories, Burlingame, CA), and 1 μl SYBR-green (Molecular Probes, Eugene, OR). Slides were evaluated immediately after staining.

Hardware and Software for Image Acquisition and Comet Analysis

Fifty comets per slide were examined under an epifluorescence microscope (Axiovert 135, Zeiss, Germany; 40× air objective) equipped with an adequate set of filters for SYBR-green and a monochromator (T.I.L.L. Photonics, Munich, Germany) as a light source for the image analysis. Excitation was performed at 461 nm and emission at 510 nm. Images were acquired with a Sony Video Camera (XC-7500) and evaluated by special software for comet image analysis (VisCOMET, Impuls GmbH, Gilching, Germany).

Statistical Evaluation

In total, results from five independent experiments were analyzed to detect the dose effect of the four different types of photon radiation and three independent experiments concerning DNA temporal repair patterns. DNA damage was determined by analyzing the Olive tail moment or percentage DNA in tail. The Olive tail moment was calculated by (center of gravity of tail profile − center of gravity of head profile) × tail intensity/total intensity and expressed in arbitrary units since length calibration is defined in pixels rather than micrometers.

The original data set was computed in box plots (Statistica Version 6, StatSoft). The data were transformed to natural logarithms to achieve a greater degree of normality in the data set distributions. The justification for the use of such natural logarithm transformations to achieve a greater degree of normality in the distribution function for tail moment is given in the Appendix. Linear fits by multiple regression analysis were applied to the dose–response curves.

RESULTS

A clear dose–response relationship for initial DNA damage was observed in human lymphocytes exposed to 29 kV X rays and the reference radiation types within the dose range from 0.5 to 3 Gy. As shown in Fig. 2, the results for the two damage parameters analyzed, tail moment and percentage DNA in tail, are rather similar and are not normally distributed. The tail moment values were transformed by natural logarithms for all five independent experiments (Fig. 3a), while for percentage DNA in tail, means of 50 individual cells for five independent experiments were computed (Fig. 3b). There were only minor variations in the values obtained in the different experiments. The best-fit parameters indicate a linear dose–response relationship for all four radiation types (Fig. 4a, b) for tail moment as well as for percentage DNA. The slopes did not differ significantly from each other over the total dose range investigated. To determine whether 29 kV X rays were able to increase DNA damage in the low-dose range, we focused on the dose range from 0 to 1 Gy (Fig. 5). In this case too, the slopes did not differ significantly from each other. When tested by multiple regression analysis with the overparameterized coding method and separate slope design (Table 1), no significant effect could be detected amongst either the experiments or the radiation types. Since two out of five experiments were performed with blood from a female donor, the model was also investigated for gender effects.

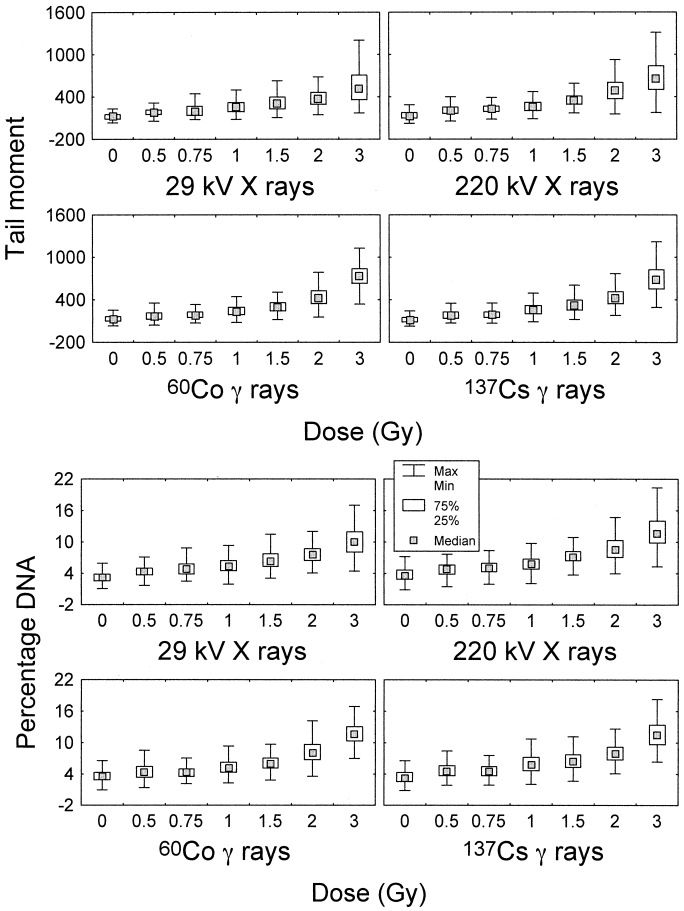

FIG. 2. Damage distribution demonstrated by box plot analyses of two damage parameters, tail moment and percentage DNA in the tail, as a function of free in air kerma dose.

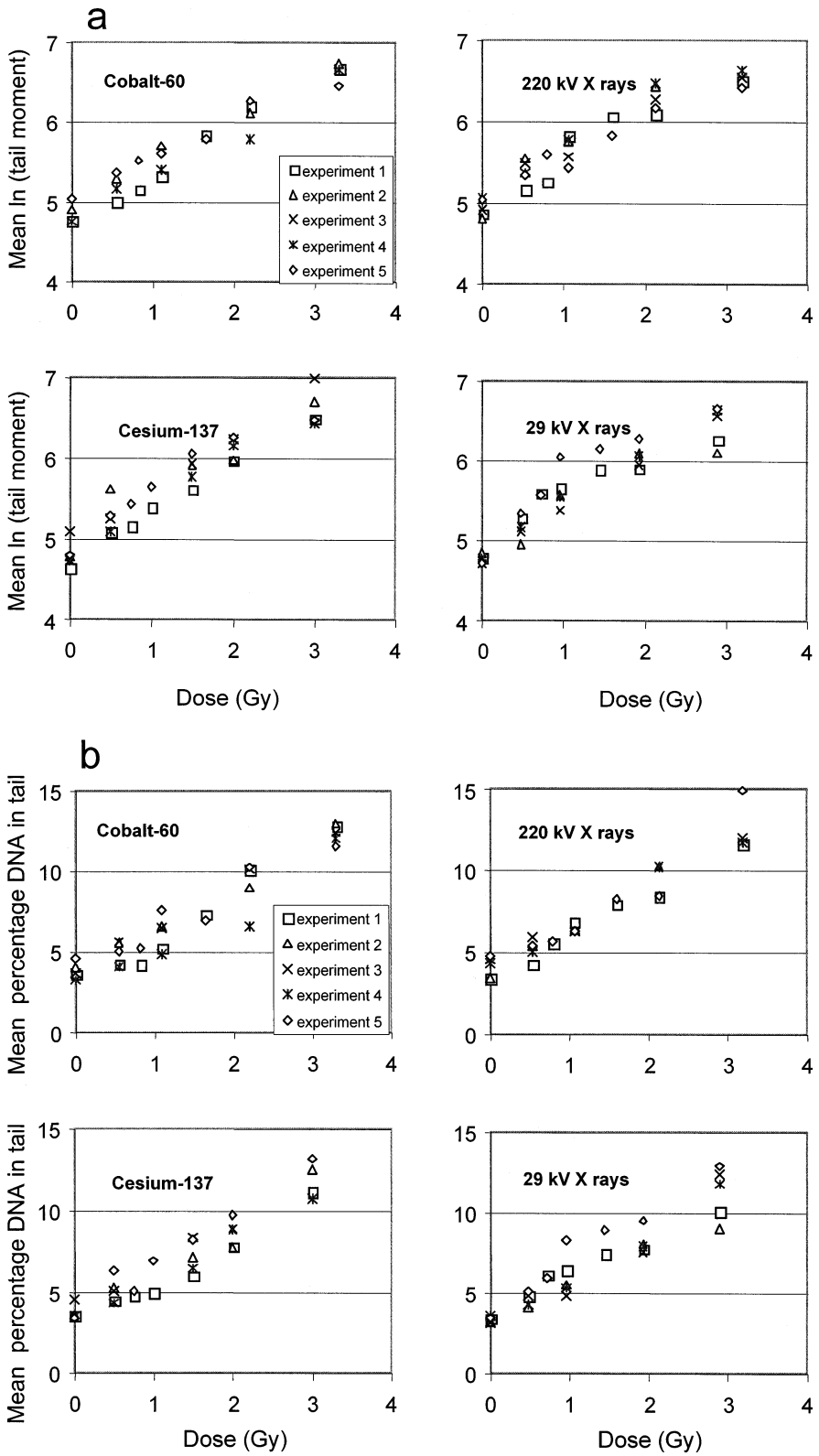

FIG. 3. Panel a: The mean natural logarithm of the tail moment as a function of blood dose for four different types of photon radiation. Each mean was computed from 50 individual ln(tail moment) values. Panel b: The mean percentage DNA in tail as a function of blood dose for four different types of photon radiation. Each mean was computed from 50 individual values.

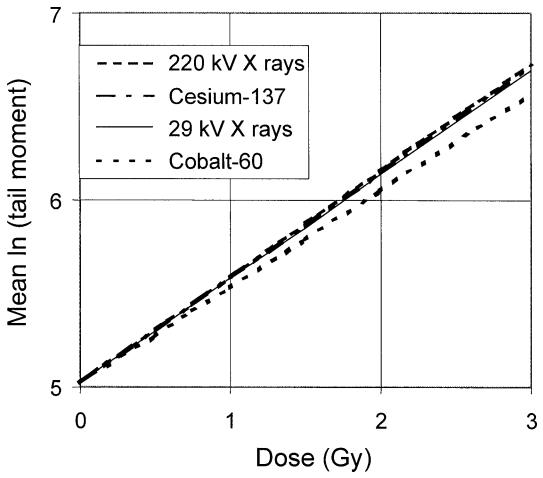

FIG. 4. Best-fit lines from the multiple regression for mean ln(tail moment) as a function of mean blood dose and as detailed in Table 1. The slopes are not significantly different; the intercept shown is for one experiment.

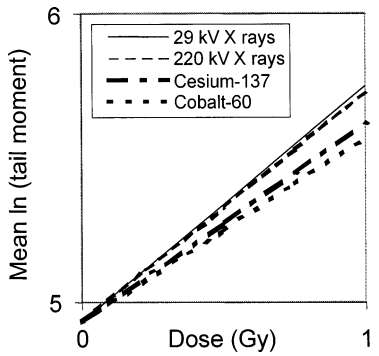

FIG. 5. The best-fit lines from a similar regression to that described in Table 1 but with a restricted mean blood dose range of 0 to 1 Gy. The trends in gradient are different from above, but not statistically significantly so. The intercept shown is for one experiment

No significant effect of this parameter on the data could be detected.

After irradiation of blood cells with an air kerma dose of 3 Gy, DNA repair was investigated after set intervals of 10, 20, 30 and 60 min. The experiments were repeated three times. The fraction of remaining damage was calculated by subtraction of the control tail moment from the corresponding tail moment at the various times. Initial damage at time zero was set to 100%. High variation in the experimental data can be seen during the fast repair period during the first 20 min after irradiation (Fig. 6). At repair times longer than 20 min, the residual damage showed only minor interexperimental differences. The best-fit calculation for the results obtained for the four radiation types did not detect any significant difference for the remaining damage after 60 min or for the repair half-time (Tables 2 and 3). However, there was a tendency that for irradiation with 29 kV X rays, repair of damaged DNA proceeded slightly more slowly in the first 10 to 20 min compared to the other reference radiation types (Fig. 7). In this time range, the experimental data are so variable that, for the X rays, a difference in half-time of only about 7 min [$1.645 \times (2.84 + 1.53)$] would have been detected in the fit function parameters with 90% confidence. This is because of the many sources of uncertainty due to dosimetry errors and intraexperimental and interexperimental variation.

DISCUSSION

The present study examines, for the first time, at the single cell level, the initial DNA damage and the subsequent time-dependent DNA repair in human lymphocytes after irradiation with photons of different energies. The comet assay data did not indicate any difference in the initial radiation damage produced by 29 kV X rays relative to the reference radiations, i.e. 220 kV X rays and ^{137}Cs and ^{60}Co γ rays, either for the total dose range or in the low-dose range. It appeared that the 29 kV X rays tended to slow down DNA repair more than the reference radiation types, but this effect was not significant.

These results are, with some restrictions, consistent with physical examinations and predictions concerning, for ex-

TABLE 1
Multiple Regression with the Overparameterized Coding Method and Separate Slope Design: Results for the Categorical (Radiation Type and Experiment Number) and Continuous (Mean Blood Dose) Predictor Variables with Interaction between Dose and Radiation Type

Parameter	Best estimate	Standard error	*t* ratio
a	5.019	0.040	124.582
b_1	0.557	0.025	21.867
b_2	0.011	0.029	0.382
b_3	−0.040	0.029	−1.409
b_4	0.009	0.030	0.297
b_5	−0.145	0.049	−2.969
b_6	−0.033	0.053	−0.627
b_7	−0.028	0.053	−0.518
b_8	−0.103	0.053	−1.930

Standard error of mean ln(tail moment)	0.182
Coefficient of determination	0.917
df	107
F value	147.35
SS regression	39.12
SS residual	3.55

Notes. The model is: mean ln(tail moment) = $a + x_1 (b_1 + b_2x_2 + b_3x_3 + b_4x_4) + b_5x_5 + b_6x_6 + b_7x_7 + b_8x_8$, where x_1 is the mean blood dose in grays; x_2 is either 0 or 1 and indicates a differential effect of 220 kV X rays relative to 29 kV X rays, x_3 is either 0 or 1 and indicates a differential effect of ^{60}Co relative to 29 kV X rays, x_4 is either 0 or 1 and indicates a differential effect of ^{137}Cs relative to 29 kV X rays, x_5 is either 0 or 1 and indicates a differential effect of experiment 1 relative to experiment 5, x_6 is either 0 or 1 and indicates a differential effect of experiment 2 relative to experiment 5, x_7 is either 0 or 1 and indicates a differential effect of experiment 3 relative to experiment 5, x_8 is either 0 or 1 and indicates a differential effect of experiment 4 relative to experiment 5. The various sums of squares (SS) and degrees of freedom (*df*) are given with the other usual measures for goodness of fit.

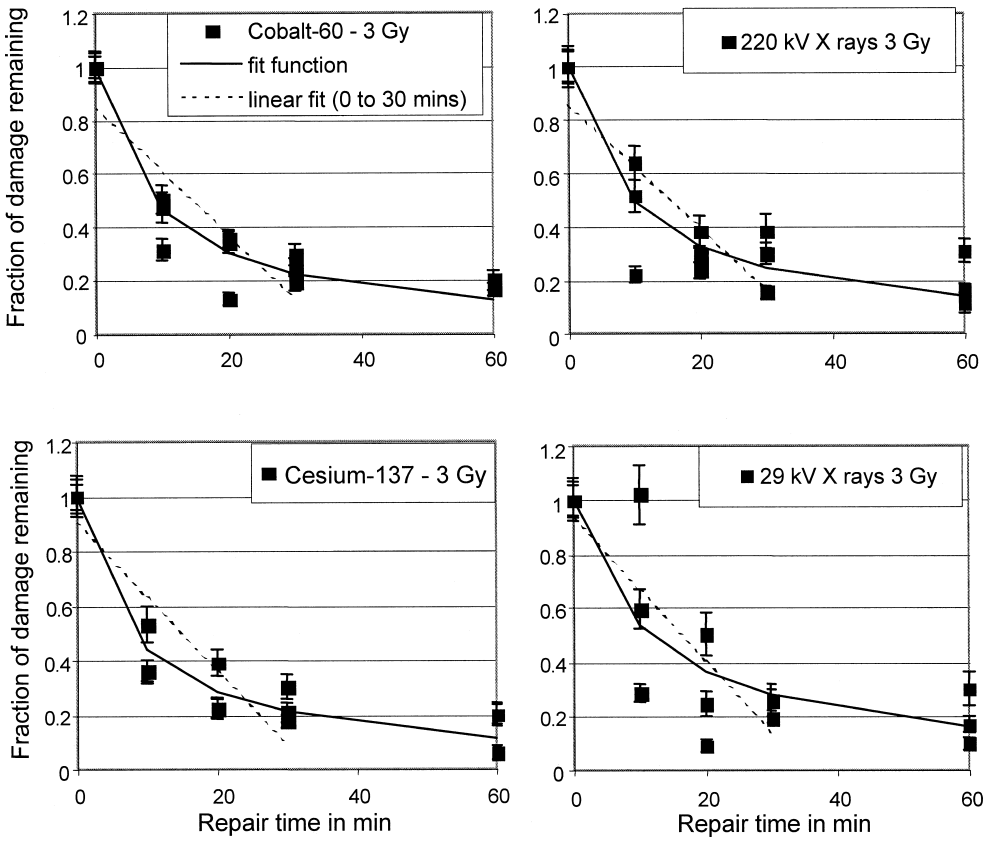

FIG. 6. The fraction of damage, mainly due to single-strand breaks, remaining after an initial irradiation with a free-in-air kerma dose of 3 Gy for four radiation types and for various repair times. Two points almost coincide for ^{137}Cs γ rays at 10, 20 and 60 min repair time.

ample, the assessment of the possible difference in effectiveness between mammography X rays and conventional X rays. As stated by Kellerer (*9*), Kellerer and Chen (*10*), and the ICRP (*38*), an analysis in terms of the explicit electron spectra at different photon energies leads to the conclusion that the RBE of mammography X rays compared with conventional X rays will, regardless of the underlying mechanisms, be between 1 and 2; this includes a consideration of a potential contribution of the 0.5 keV Auger electrons from oxygen that accompany all photoelectrons in water but only a minority of the Compton electrons that predominate at the higher photon energies. This suggestion is well in line with the RBE of about 1.3, as deduced by Brenner and Amols (*11*) from microdosimetric data. This very low RBE value for primary lesions may be responsible for the present observation of a tendency of slowing down DNA repair after exposure of human lymphocytes to mammography X rays, indicating more complex DNA damage than after exposure to conventional X rays. The present analysis, which primarily assessed single-strand breaks, was consistent with the recent microdosimetric results. However, the present results are not consistent with recent reports (*1–8*, *39*) that mammography X rays are more than twice as effective as conventional X rays or γ rays at intermediate doses or even more effective at small doses. There are two plausible explanations for this disparity: (1)

TABLE 2
Results of the Best Least-Squares Linear Fit Parameters for the Repair Time Data between 0 and 30 min as Displayed in Fig. 5

Radiation type	Gradient	SE of gradient	Intercept	SE of intercept	χ^2	*df*	*P*	α	$T_{1/2}$ (min)
29 kV X rays	−0.0265	0.0055	0.93	0.10	0.46	10	1	4×10^{-6}	16.41
220 kV X rays	−0.0232	0.0048	0.86	0.09	0.34	10	1	1×10^{-6}	15.40
^{60}Co γ rays	−0.0242	0.0044	0.85	0.08	0.29	10	1	5×10^{-7}	14.44
^{137}Cs γ rays	−0.0270	0.0043	0.90	0.08	0.15	10	1	2×10^{-8}	14.97

Note. The fit function was F_d = gradient × t + intercept, where F_d is the fraction of damage remaining and t is the time allowed for repair in minutes.

TABLE 3
Results of the Best Least-Squares Fit Parameters for the Repair Time Data between 0 and 60 min as Displayed Separately in Fig. 5 and Together in Fig. 6

Radiation type	A	SE of A	χ^2	df	P	α
29 kV X rays	11.52	2.84	0.44	13	1	2.5×10^{-8}
220 kV X rays	9.62	1.53	0.17	13	1	5×10^{-11}
^{60}Co γ rays	8.50	1.02	0.09	13	1	8.5×10^{-13}
^{137}Cs γ rays	8.00	0.85	0.07	13	1	1.4×10^{-13}

Notes. The fit function was $F_d = A/(t + A)$, where F_d is the fraction of damage remaining at t, the time allowed for repair in minutes. The major advantage of this parameterization is that there is only one fitted parameter, and this is designed to be the repair half-time in minutes.

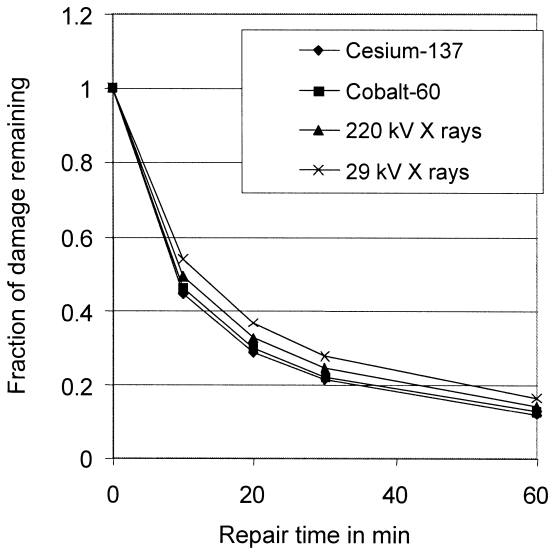

FIG. 7. The best fit to the fraction of damage remaining after irradiation with 3 Gy free-in-air kerma photon radiation as a function of repair time between 0 and 60 min (also displayed separately in Fig. 6). The fit function was $Fd = A/(t + A)$, where Fd is the fraction of damage remaining at t, the time allowed for repair in minutes. The major advantage of this parameterization is that there is only one fitted parameter, and this is designed to be the repair half-time in minutes.

The biologically relevant DSBs are masked by the prevailing SSBs, since DSBs contribute only about 2% to the total amount of breakage. If 29 kV X rays produce more DSBs by a factor of 2–4, this would not be detectable in the experimental system applied here, but it could be responsible for the delayed repair kinetics observed here for the 29 kV X rays. (2) On the other hand there are no, or only minor, differences in RBE for the initial biological effects, the quantity of primary lesions in DNA as detected by the comet assay, compared to the later effects detected by other assays. However, the higher RBE values obtained in studies of later biological damage indicators within the complete biological effectiveness range, i.e. from the photon-induced initial DNA damage to the late radiation effects in humans may then be due to the involvement of cellular processes acting on DNA as the first target of exposure to ionizing radiation. Measurements of the initial yield of DNA DSBs as a function of LET indicated only modest increases of 2–3, even at LETs that have an RBE for cell killing as high as 10, but when comparing the ratio of point mutations, high-LET radiation produces 12 times more. Thus Ward (*40*) suggested mechanisms whereby complex damage to intracellular DNA is caused by multiple radical attacks on local sites producing locally multiply damaged sites or clustered lesions. He concluded that the higher RBE for cell killing must be associated with the cell's response to the initial damage. Tanaka *et al.* (*31*) compared results from both the comet assay and studies of chromosomal aberrations and found the latter to be two to three times more sensitive and in good agreement with results from cell transformation experiments. They also suggested that primary DNA damage is amplified during cell proliferation after irradiation. If repaired, even in SSBs that are offset by several base pairs, loss of sequence information may occur and thus lead to errors in base sequences (*41*). A recent investigation (*42*) demonstrates that during DNA replication abasic sites, which are also created during radiation exposure, may result in the loss of a base triplet and give rise to proteins lacking a single amino acid. Proteins lacking a single amino acid have been implicated in cancer and other diseases in which oxidative stress is a causative factor. Thus different repair pathways and DNA replication are steps in the downstream processing where initial DNA damage may be amplified.

CONCLUSION

The results from the present comet assay experiments illustrate that the yields of the initial DNA damage in human lymphocytes exposed to 29 kV X rays (mammography X rays) do not differ significantly from the corresponding yields obtained simultaneously for conventional X rays or ^{137}Cs and ^{60}Co γ rays. Especially because of the revived debate on the different magnitudes of the biological effects induced by photons with different energies, it is important to obtain information on the relative effects of low photon energy and reference radiations such as higher-energy X rays or γ rays. The present results are in essence consistent with physical models concerning the primary lesions at the DNA. On the other hand, it has long been recognized that, especially at different low doses, low-LET radiation types do not have the same biological effectiveness. In chromosome aberrations or cell transformation studies, there can be some biological factors that enhance the difference between mammography X rays and the reference radiation types. These differences in the downstream processing of primary lesions to produce late radiation effects lead to different RBE values.

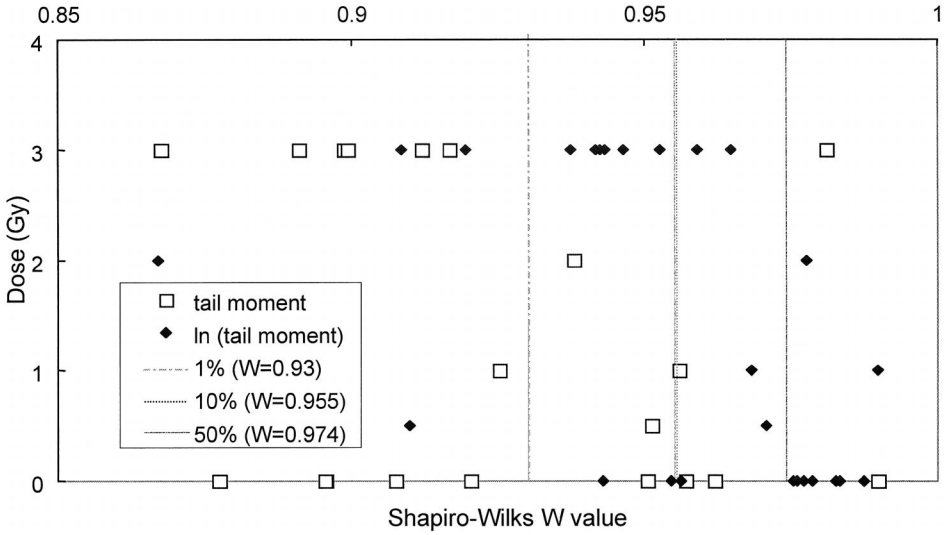

FIG. A1. Results for 52 *W* tests, 26 for tail moment and 26 for ln(tail moment); the percentage points are also represented as three vertical lines. Plotted values of *W* to the right of the vertical lines can be accepted for the hypothesis of normality at one of the three percentage points given. Critical values for normality hypothesis testing for $n = 50$ are $W = 0.93$, 0.955 and 0.974 for the percentage points 1, 10 and 50, respectively.

APPENDIX

The Underlying Distribution for Tail Moment

Each of the points in Fig. 3 represents the mean value of $n = 50$ individual ln(tail moment) values, one from each cell. There are 96 such sets of 50 data points contributing to Fig. 3, and part of the data analysis procedure involved identifying the best representation of the underlying distribution. A qualitative assessment of some of the individual distributions revealed a wide spectrum of shapes including symmetrical, skewed and weakly bimodal. Previous work has identified the form to be best represented by log-normal (*43*) or χ^2 (*44*).

To assess the statistical form for the present data sets, a detailed analysis has been done for a subset of the data for one experiment from the middle of the data collection process and the two types of X radiation. This reduced the analysis to 26 data sets on which tests of normality for both tail moment and ln(tail moment) were performed (52 tests). Initially a χ^2 test was performed and indicated that the distributions were closer to log-normal than normal. However, the disadvantage of the χ^2 test for normality is that the data must be grouped, and with 50 points the maximum number of bins allowed is only 10. A comparative study of various tests for normality (*45*) has evaluated the sensitivity of nine different tests and found the Shapiro-Wilks *W* test (*46*) to provide a generally superior measure of non-normality. The necessary Shapiro-Wilks *W* coefficients and percentage points for hypothesis testing for $n = 50$ are readily available in the literature (*46*), and this test was considered suitable for application to the comet assay data. The *W* statistic is obtained by dividing two different estimators for the variance, i.e. the squared slope of the probability plot regression line and the usual symmetric sample sum of squares about the mean, which should both be very similar for a normal distribution and result in *W* values close to unity, for $n = 50$, $0.14 < W \leq 1$. Small values of *W* are significant, i.e. indicate non-normality. Critical values for normality hypothesis testing for $n = 50$ are $W = 0.93$, 0.955 and 0.974 for the percentage points 1, 10 and 50, respectively.

Results for 52 *W* tests, 26 for tail moment and 26 for ln(tail moment), are presented in Fig. A1, where the percentage points are also represented as three vertical lines. Plotted values of *W* to the right of the vertical lines can be accepted for the hypothesis of normality at one of the three percentage points given. The choice of dose for the ordinate is not to indicate a dose response but merely to spread out the points better in the graphical representation. The general trend is that more ln(tail moment) tests can be accepted as normal than the corresponding tests for tail moment; i.e., there are more diamonds than open squares toward the right hand side of the graph. In fact, there are five tail moment *W*-test values off the scale below $W = 0.85$. The hypothesis that the distribution is normal can be rejected in a larger number of cases for tail moment than for ln(tail moment). On the basis of these results, it was concluded that the underlying distribution of tail moment was more closely represented by log-normal than by normal.

ACKNOWLEDGMENTS

The authors would like to thank I. Baumgartner and S. Widemann for technical assistance, Dr. M. Asmuss for experimental support, and Dr. W. Rühm and Dr. A. Friedl for useful and enlightening discussions.

Received: August 16, 2004; accepted: December 9, 2004

REFERENCES

1. D. Frankenberg, K. Kelnhofer, I. Garg, K. Bar and M. Frankenberg-Schwager, Enhanced mutation and neoplastic transformation in human cells by 29 kVp relative to 200 kVp X rays indicating a strong dependence of RBE on photon energy. *Radiat. Prot. Dosim.* **99**, 261–264 (2002).
2. E. Schmid, D. Regulla, H. M. Kramer and D. Harder, The effect of 29 kV X rays on the dose response of chromosome aberrations in human lymphocytes. *Radiat. Res.* **158**, 771–777 (2002).
3. E. Schmid, M. Krumrey, G. Ulm, H. Roos and D. Regulla, The maximum low-dose RBE of 17.4 and 40 keV monochromatic X rays for the induction of dicentric chromosomes in human peripheral lymphocytes. *Radiat. Res.* **160**, 499–504 (2003).
4. W. Göggelmann, C. Jacobsen, W. Panzer, L. Walsh, H. Roos and E. Schmid, Re-evaluation of the RBE of 29 kV x-rays (mammography x-rays) relative to 220 kV x-rays using neoplastic transformation of human CGL1-hybrid cells. *Radiat. Environ. Biophys.* **42**, 175–182 (2003).
5. R. Cox, J. Thacker and D. T. Goodhead, Inactivation and mutation of cultured mammalian cells by aluminium characteristic ultrasoft X-rays. II. Dose-responses of Chinese hamster and human diploid cells to aluminium X-rays and radiations of different LET. *Int. J. Radiat. Biol.* **31**, 561–576 (1977).
6. C. Borek, E. J. Hall and M. Zaider, X rays may be twice as potent

as gamma rays for malignant transformation at low doses. *Nature* **301**, 156–158 (1983).

7. L. Hieber, K. Trutschler, J. Smida, M. Wachsmann, G. Ponsel and A. M. Kellerer, Radiation-induced cell transformation: Transformation efficiencies of different types of ionizing radiation and molecular changes in radiation transformants and tumor cell lines. *Environ. Health Perspect.* **88**, 169–174 (1990).

8. D. Frankenberg, H. Kuhn, M. Frankenberg-Schwager, W. Lenhard and S. Beckonert, 0.3 keV carbon K ultrasoft X-rays are four times more effective than gamma-rays when inducing oncogenic cell transformation at low doses. *Int. J. Radiat. Biol.* **68**, 593–601 (1995).

9. A. M. Kellerer, Electron spectra and the RBE of X rays. *Radiat. Res.* **158**, 13–22 (2002).

10. A. M. Kellerer and J. Chen, Comparative microdosimetry of photoelectrons and Compton electrons: An analysis in terms of generalized proximity functions. *Radiat. Res.* **160**, 324–333 (2003).

11. D. J. Brenner and H. I. Amols, Enhanced risk from low-energy screen-film mammography x-rays. *Br. J. Radiol.* **62**, 910–914 (1989).

12. K. Eguchi, T. Inada, M. Yaguchi, S. Satoh and I. Kaneko, Induction and repair of DNA lesions in cultured human melanoma cells exposed to a nitrogen-ion beam. *Int. J. Radiat. Biol.* **52**, 115–123 (1987).

13. J. Heilmann, H. Rink, G. Taucher-Scholz and G. Kraft, DNA strand break induction and rejoining and cellular recovery in mammalian cells after heavy-ion irradiation. *Radiat. Res.* **135**, 46–55 (1993).

14. P. E. Bryant, R. Warring and G. Ahnstrom, DNA repair kinetics after low doses of X-rays. A comparison of results obtained by the unwinding and nucleoid sedimentation methods. *Mutat. Res.* **131**, 19–26 (1984).

15. J. H. Schwachofer, R. P. Crooijmans, H. Hoogenhout, H. B. Kal, R. Q. Schaapveld and J. Wessels, Differences in repair of radiation induced damage in two human tumor cell lines as measured by cell survival and alkaline DNA unwinding. *Strahlenther. Onkol.* **167**, 35–40 (1991).

16. D. Blocher, DNA double strand breaks in Ehrlich ascites tumour cells at low doses of x-rays. I. Determination of induced breaks by centrifugation at reduced speed. *Int. J. Radiat. Biol.* **42**, 317–328 (1982).

17. M. A. Ritter, J. E. Cleaver and C. A. Tobias, High-LET radiations induce a large proportion of non-rejoining DNA breaks. *Nature* **266**, 653–655 (1977).

18. K. Yamada, Y. Kameyama and S. Inoue, An improved method of alkaline sucrose density gradient sedimentation to detect less than one lesion per 1 Mb DNA. *Mutat. Res.* **364**, 125–131 (1996).

19. J. Dahm-Daphi and E. Dikomey, Rejoining of DNA double-strand breaks in X-irradiated CHO cells studied by constant- and graded-field gel electrophoresis. *Int. J. Radiat. Biol.* **69**, 615–621 (1996).

20. D. Frankenberg, H. J. Brede, U. J. Schrewe, C. Steinmetz, M. Frankenberg-Schwager, G. Kasten and E. Pralle, Induction of DNA double-strand breaks by ^{1}H and ^{4}He ions in primary human skin fibroblasts in the LET range of 8 to 124 keV/micrometer. *Radiat. Res.* **151**, 540–549 (1999).

21. D. P. Garwood, L. L. Thompson and W. C. Dewey, Use of pulsed-field gel electrophoresis to measure X-ray-induced double-strand breaks in DNA substituted with BrdU. *Radiat. Res.* **128**, 210–215 (1991).

22. K. J. Weber and M. Flentje, Lethality of heavy ion-induced DNA double-strand breaks in mammalian cells. *Int. J. Radiat. Biol.* **64**, 169–178 (1993).

23. L. Weglarz, A. Koceva-Chyla, M. Drozdz and Z. Jozwiak, Single-strand breaks and repair in nuclear DNA in the presence of hydralazine assayed by the nucleoid technique. *Biochem. Mol. Biol. Int.* **43**, 513–519 (1997).

24. G. Ahnstrom, Techniques to measure DNA single-strand breaks in cells: A review. *Int. J. Radiat. Biol.* **54**, 695–707 (1988).

25. A. R. Collins, The comet assay. Principles, applications, and limitations. *Methods Mol. Biol.* **203**, 163–177 (2002).

26. P. L. Olive, DNA damage and repair in individual cells: Applications of the comet assay in radiobiology. *Int. J. Radiat. Biol.* **75**, 395–405 (1999).

27. P. L. Olive, The comet assay. An overview of techniques. *Methods Mol. Biol.* **203**, 179–194 (2002).

28. R. R. Tice, E. Agurell, D. Anderson, B. Burlinson, A. Hartmann, H. Kobayashi, Y. Miyamae, E. Rojas, J. C. Ryu and Y. F. Sasaki, Single cell gel/comet assay: Guidelines for *in vitro* and *in vivo* genetic toxicology testing. *Environ. Mol. Mutagen.* **35**, 206–221 (2000).

29. N. Gajendiran, K. Tanaka and N. Kamada, Comet assay to sense neutron 'fingerprint'. *Mutat. Res.* **452**, 179–187 (2000).

30. R. Mustonen, G. Bouvier, G. Wolber, M. Stohr, P. Peschke and H. Bartsch, A comparison of gamma and neutron irradiation on Raji cells: Effects on DNA damage, repair, cell cycle distribution and lethality. *Mutat. Res.* **429**, 169–179 (1999).

31. K. Tanaka, N. Gajendiran, S. Endo, K. Komatsu, M. Hoshi and N. Kamada, Neutron energy-dependent initial DNA damage and chromosomal exchange. *J. Radiat. Res.* **40**, 36–44 (1999).

32. I. Testard and L. Sabatier, Assessment of DNA damage induced by high-LET ions in human lymphocytes using the comet assay. *Mutat. Res.* **448**, 105–115 (2000).

33. E. Schmid, D. Schlegel, S. Guldbakke, R. P. Kapsch and D. Regulla, RBE of nearly monoenergetic neutrons at energies of 36 keV–14.6 MeV for induction of dicentrics in human lymphocytes. *Radiat. Environ. Biophys.* **42**, 87–94 (2003).

34. *European Protocol on Dosimetry in Mammography*. EUR-16263, European Commission, Brussels, 1996.

35. J. H. Hubbel, Photon mass attenuation and energy-absorption coefficients from 1 keV to 20 MeV. *Int. J. Appl. Radiat. Isot.* **33**, 1269–1290 (1982).

36. N. P. Singh, M. T. McCoy, R. R. Tice and E. L. Schneider, A simple technique for quantitation of low levels of DNA damage in individual cells. *Exp. Cell. Res.* **175**, 184–191 (1988).

37. N. P. Singh, R. R. Tice, R. E. Stephens and E. L. Schneider, A microgel electrophoresis technique for the direct quantitation of DNA damage and repair in individual fibroblasts cultured on microscope slides. *Mutat. Res.* **252**, 289–296 (1991).

38. ICRP, *Relative Biological Effectiveness (RBE), Quality Factor (Q), and Radiation Weighting Factor (wR)*. Publication 92, *Annals of the ICRP*, Vol. 33, Pergamon Press, Oxford, 2003.

39. D. Frankenberg, K. Kelnhofer, K. Bar and M. Frankenberg-Schwager, Enhanced neoplastic transformation by mammography X rays relative to 200 kVp X rays: Indication for a strong dependence on photon energy of the RBE_M for various end points. *Radiat. Res.* **157**, 99–105 (2002).

40. J. F. Ward, The complexity of DNA damage: Relevance to biological consequences. *Int. J. Radiat. Biol.* **66**, 427–432 (1994).

41. A. A. Francis, R. D. Snyder, W. C. Dunn and J. D. Reagan, Classification of chemical agents as to their ability to induce long- or short-patch DNA repair in human cells. *Mutat. Res.* **83**, 159–169 (1981).

42. K. M. Kroeger, J. Kim, M. F. Goodman and M. M. Greenberg, Effects of the C4′-oxidized abasic site on replication in *Escherichia coli*. an unusually large deletion is induced by a small lesion. *Biochemistry* **43**, 13621–13627 (2004).

43. E. Bauer, R-D. Recknagel, U. Fiedler, L. Wollweber, C. Bock and K. O. Greulich, The distribution of the tail moments in single cell gel electrophoresis (comet assay) obeys a chi-square (χ^2) not a gaussian distribution. *Mutat. Res.* **398**, 101–110 (1998).

44. S. J. Wiklund and E. Agurell, Aspects of design and statistical analysis in the comet assay. *Mutagen* **18**, 167–175 (2003).

45. S. S. Shapiro, M. B. Wilk and H. J. Chen, A comparative study of various tests for normality. *J. Am. Stat. Assoc.* **63**, 1343–1372 (1968).

46. S. S. Shapiro and M. B. Wilks, An analysis of variance test for normality (complete samples). *Biometrika* **52**, 591–611 (1965).